frontiers in Immunology

The NF-?B RelA transcription factor is critical for regulatory T cell activation and stability

Emilie Ronin[1], Martina Lubrano di Ricco[1], Romain Vallion[1], Jordane Divoux[1], Ho-keun Kwom[2], Sylvie Grégoire[1], Davi Collares[3], Angeline Rouers[1], Véronique Baud[3], Christophe Benoist[2], Benoit L. Salomon[1*]

[1]INSERM U1135 Centre d'Immunologie et de Maladies Infectieuses, France, [2]Division of Immunology, Department of Immunology and Microbiology, Harvard Medical School, United States, [3]Université Paris Descartes, France

Submitted to Journal:
Frontiers in Immunology

Specialty Section:
T Cell Biology

ISSN:
1664-3224

Article type:
Original Research Article

Received on:
16 Jun 2019

Accepted on:
04 Oct 2019

Provisional PDF published on:
04 Oct 2019

Frontiers website link:
www.frontiersin.org

Citation:
Ronin E, Lubrano_di_ricco M, Vallion R, Divoux J, Kwom H, Grégoire S, Collares D, Rouers A, Baud V, Benoist C and Salomon BL(2019) The NF-κB RelA transcription factor is critical for regulatory T cell activation and stability. *Front. Immunol.* 10:2487. doi:10.3389/fimmu.2019.02487

The NF-κB RelA transcription factor is critical for regulatory T cell activation and stability

Emilie Ronin[1], Martina Lubrano di Ricco[1], Romain Vallion[1], Jordane Divoux[1], Ho-Keun Kwon[3], Sylvie Grégoire[1], Davi Collares[2], Angéline Rouers[1], Véronique Baud[2], Christophe Benoist[3] and Benoit L Salomon[1*]

[1]Sorbonne Universités, UPMC Univ Paris 06, INSERM, CNRS, Centre d'Immunologie et des Maladies Infectieuses (CIMI-Paris), Paris, France.

[2]Laboratoire NF-κB, Differentiation and Cancer, Université Paris Descartes, Sorbonne Paris Cité, Paris, France.

[3]Division of Immunology, Department of Microbiology and Immunobiology, Harvard Medical School, Boston, MA 02115.

[*]Corresponding author

Correspondence should be addressed to B.L.S. (benoit.salomon@upmc.fr)

#words: 6851

#figures: 7

ABSTRACT

Regulatory T cells (Tregs) play a major role in immune homeostasis and in the prevention of autoimmune diseases. It has been shown that c-Rel is critical in Treg thymic differentiation, but little is known on the role of NF-κB on mature Treg biology. We thus generated mice with a specific knockout of RelA, a key member of NF-κB, in Tregs. These mice developed a severe autoimmune syndrome with multi-organ immune infiltration and high activation of lymphoid and myeloid cells. Phenotypic and transcriptomic analyses showed that RelA is critical in the acquisition of the effector Treg state independently of surrounding inflammatory environment. Unexpectedly, RelA-deficient Tregs also displayed reduced stability and cells that had lost Foxp3 produced inflammatory cytokines. Overall, we show that RelA is critical for Treg biology as it promotes both the generation of their effector phenotype and the maintenance of their identity.

KEYWORDS

Regulatory T cells, NF-κB, autoimmunity, stability, activation

INTRODUCTION

CD4$^+$ CD25$^+$ Foxp3$^+$ regulatory T cells (Tregs) play a critical role in immune homeostasis and in the prevention of autoimmune diseases by regulating immune responses (Sakaguchi et al. 2006). In humans and mice, it is well established that *forkhead box protein 3* (*Foxp3)* deficiency conducts to the development of an autoimmune syndrome leading to early death. Although *Foxp3* plays a critical role in the differentiation, suppressive function and stability of Tregs, other transcription factors (TFs), some of which interacting with Foxp3 in multi-molecular complexes, are also involved in different aspects of their biology. Some, such as c-Rel, are involved in Treg differentiation (Isomura et al. 2009; Long et al. 2009). Others, such as NFAT, RunX1, BACH2 or Eos are critical to maintain their suppressive activity (Wu et al. 2006; Ono et al. 2007; Pan et al. 2009; Roychoudhuri et al. 2013). Another group of TFs, including Blimp1, Myb, STAT3, Tbet, IRF4, Bcl6 or PPARg are involved in further differentiation of activated Tregs and in their capacity to suppress different types of immune responses (Chaudhry et al. 2009; Koch et al. 2009; Zheng et al. 2009; Cretney et al. 2011; Linterman et al. 2011; Cipolletta et al. 2012; Dias et al. 2017). Finally, STAT5, TET, GATA3, p300/CBP, Blimp1 or Ezh2 have been shown to maintain Treg identity and stability by controlling Foxp3 transcription and epigenetics (Wohlfert et al. 2011; Feng et al. 2014; Liu et al. 2014; DuPage et al. 2015; Yang et al. 2015; Garg et al. 2019). Although it has been reported that NF-κB is able to bind to the regulatory sequence of *Foxp3* and to interact with a complex containing Foxp3 (Bettelli, Dastrange, et Oukka 2005; Isomura et al. 2009; Long et al. 2009), its role in Treg biology needs to be further analyzed.

The NF-κB TFs consist of homo or heterodimeric molecules of NF-κB1 (p105/50), RelA (p65) and c-Rel subunits for the canonical pathway and of NF-κB2 (p100/52) and RelB subunits for the non-canonical pathway. It has been reported that c-Rel is essential for thymic Treg

development by binding to the promoter sequence and the conserved non-coding sequence (CNS) 3 of *Foxp3* (Isomura et al. 2009; Long et al. 2009; Ruan et al. 2009). The role of NF-κB in mature Treg biology has been addressed by knocking-out upstream activators of the pathway, such as IKKα and IKKß kinases. Mice with a conditional knockout (KO) in Tregs of either Ubc13, an E2 ubiquitin ligase activating IKKβ, or of IKKβ itself, develop a spontaneous autoimmune syndrome, associated with conversion of Tregs into effector-like T cells without Foxp3 loss or reduced Treg survival, respectively (Chang et al. 2012; Heuser et al. 2017). Mice with a conditional KO of IKKα in $CD4^+$ T cells have a decreased proportion of Tregs in lymphoid organs, which seem to have a defective suppression and proliferation capacities *in vivo* (Chen et al. 2015). The specific role of RelA in Tregs, which is considered as the main factor of NF-κB members in conventional T cells (Oh et Ghosh 2013), has been recently studied. By interacting with RelA and other TFs, such as Helios and p300, Foxp3 forms a multimolecular complex localized in active nuclear areas to act primary as a transcriptional activator (Kwon et al. 2017). Mice with a conditional KO of RelA in Tregs develop a severe and early spontaneous autoimmune syndrome that is associated with a defect of effector Tregs (Messina et al. 2016; Vasanthakumar et al. 2017; Oh et al. 2017). Here, we confirmed these latter findings and added further information on the nature of the disease with extensive description of lymphoid and myeloid cell activation in lymphoid and non-lymphoid tissues. Importantly, we revealed that RelA-deficient Tregs were unstable, lost Foxp3 expression and produced inflammatory cytokines, highlighting that RelA is also critical to maintain Treg stability and identity.

RESULTS

Conditional ablation of RelA in Tregs leads to the development of a spontaneous autoimmune syndrome

To assess the role of RelA in Treg biology, we generated *Foxp3*^{Cre} *Rela*^{lox} mice that have a specific deletion of RelA in Tregs by crossing mice expressing CRE in Tregs with mice expressing a *Rela* floxed allele. In these *Foxp3*^{Cre} *Rela*^{lox} mice, Tregs expressed a non-functional truncated form of RelA (Fig. 1A), as expected using this floxed allele (Algül et al. 2007). From 5-10 weeks of age, *Foxp3*^{Cre} *Rela*^{lox} mice developed a spontaneous disease characterized by localized alopecia and skin lesions (epidermal hyperplasia, hyperparakeratosis, cystic hair), and reduced weight gain compared to *Foxp3*^{Cre} control mice (Fig. 1B, C). This pathology had high penetrance and was severe since most of the animals had to be sacrificed for ethical reasons by 45 weeks of age (Fig. 1D, E). At 10-12 weeks of age, *Foxp3*^{Cre} *Rela*^{lox} mice exhibited adenomegaly and macroscopic signs of mild colon inflammation (Fig. 1F, G). Histological analyses showed moderate immune cell infiltration in the lung, stomach and colon and high level of immune cell infiltration in the skin (Fig. 1H). The liver and small intestine were not or minimally infiltrated. Thus, mice with RelA-deficient Tregs developed a severe and systemic inflammatory syndrome.

We started the characterization of this syndrome by analyzing the lymphocyte compartment of 10-12 week-old *Foxp3*^{Cre} *Rela*^{lox} mice. Numbers of CD45^{+} leukocytes were highly increased in the skin draining lymph nodes (sdLN), the internal LN (iLN, corresponding to pancreatic and paraaortic LN) and the inflamed non-lymphoid tissues (lung and skin) but not in the spleen, mesenteric LN (mLN) or the non-inflamed non-lymphoid tissues (liver, small intestine) (Fig. 2A). This leukocyte expansion was due to increased numbers of CD8^{+} and CD4^{+} T cells, B cells (Fig. 2B and data not shown) and myeloid cells (see below). Moreover, the proportions of

115 $CD44^{high}CD62L^{low}$, $ICOS^+$ and $Ki67^+$ activated/memory $CD8^+$ and $CD4^+$ conventional T cells
116 were significantly increased in the spleen, sdLN and lung of *Foxp3*^{Cre} *Rela*^{lox} mice compared
117 to *Foxp3*^{Cre} control mice (Fig. 2C, D and Sup. Fig. 1A). The same tendency was observed in
118 the colon and skin, although this was not significant, probably because basal levels of activated
119 cells were already high in *Foxp3*^{Cre} control mice. Interestingly, an increased proportion of
120 activated/memory T cells was observed in the iLN and mLN as well as in the non-inflamed
121 liver and small intestine, demonstrating a global systemic T cell activation in *Foxp3*^{Cre} *Rela*^{lox}
122 mice (Sup. Fig. 1B). Systemic inflammation was confirmed by quantifying cytokines in the
123 serum, where we observed highly increased levels of IFNγ, IL-4, IL-10, IL-17, IL-6 and TNFα
124 (Fig. 2E). Also, serum levels of IgM, IgG1, IgG2b, IgA and IgE (Fig. 2F) and of anti-DNA
125 autoantibodies (Fig. 2G) were increased in 12-14 week-old sick *Foxp3*^{Cre} *Rela*^{lox} mice
126 compared to *Foxp3*^{Cre} control mice.
127 The systemic inflammation was further documented by analyzing myeloid cells, characterized
128 as shown in Supp. Fig. 2A. Their numbers were strongly increased in the spleen and sdLN as
129 well as in the inflamed non-lymphoid tissues, lung and skin, in *Foxp3*^{Cre} *Rela*^{lox} mice compared
130 to controls (Supp. Fig. 2B). This increase of myeloid cells was due to an increase of neutrophils
131 in all these tissues and of eosinophils and monocytes in the lymphoid organs and the skin (Supp.
132 Fig. 2C). A similar trend was observed in the colon.
133 Only part of this inflammatory phenotype was observed in 4-6 week-old *Foxp3*^{Cre} *Rela*^{lox} mice.
134 Increased numbers of whole $CD45^+$ leukocytes were observed in sdLN and iLN but not yet in
135 the lung and skin (Sup. Fig. 3A). A trend for higher proportion of activated/memory T cells,
136 defined by expression of CD44, CD62L and Ki67, was observed in all analyzed lymphoid and
137 non-lymphoid tissues of young mice (Sup. Fig. 3B). Finally, inflammatory cytokines, natural
138 antibodies and anti-DNA antibodies were not or minimally increased in 4-6 week-old *Foxp3*^{Cre}
139 *Rela*^{lox} compared to control mice (Fig. 2E-G). In conclusion, *Foxp3*^{Cre} *Rela*^{lox} mice developed

a severe systemic autoimmune syndrome, already uncovered at 4-6 weeks of age, followed, 1-3 months later, by massive activation of T cells, immune infiltration of several tissues and high rise of serum inflammatory cytokines, immunoglobulins and auto-antibodies.

Tregs of *Foxp3^{Cre} Rela^{lox}* mice appear to be less stable

We then analyzed Treg homeostasis in 12 week-old *Foxp3^{Cre} Rela^{lox}* mice. Strikingly, Treg proportion was significantly increased in lymphoid organs, except in mLN, while it was decreased in the colon and skin and unchanged in the liver, lung and small intestine compared to *Foxp3^{Cre}* control mice (Fig. 3A). Interestingly, in the small intestine, colon and skin of 5 week-old *Foxp3^{Cre} Rela^{lox}* mice, Treg proportion and number (except in the skin) seemed already decreased, when compared to 12 week-old *Foxp3^{Cre} Rela^{lox}* mice (Fig. 3B, Sup. Fig. 4). The proportion of activated/memory CD44^{hi}CD62L^{low} Tregs was decreased in all LN and the liver, and the same tendency was observed in the skin. However, their proportion was unchanged in the spleen, colon and small intestine and even increased in the lung (Fig. 3C). Foxp3 and CD25 expressions were unchanged (data not shown).

The severe disease of *Foxp3^{Cre} Rela^{lox}* mice in the absence of major Treg quantitative defect suggests that Tregs may be dysfunctional. *In vitro* assays showed that RelA-deficient Tregs, purified from 5-6 week-old mice, were able to suppress proliferation of conventional T cells almost as efficiently as control Tregs (Fig. 3D). To further analyze their function, we assessed their capacity to suppress colitis induced by effector T cells transferred into lymphopenic mice, measured by weight loss and histology. Surprisingly, not only RelA-deficient Tregs were unable to control colitis but the disease was even more severe compared to mice transferred with effector T cells alone (Fig. 3E, F). This exacerbated colitis was not associated with increased number of cells from Tconv origin (CD90.1^{+} cells) or to their lower propensity to differentiate in peripheral Treg (pTregs) (Sup. Fig. 5). Instead, the severe colitis was rather due

to the fact that most RelA-deficient Tregs lost Foxp3 expression in the colon and mLN, potentially differentiating in pathogenic effector T cells (Fig. 3G). In conclusion, *Foxp3*^{Cre} *Rela*^{lox} mice had higher numbers of Tregs in lymphoid tissues (probably due to systemic inflammation) but lower numbers of Tregs in the colon and skin, which could be due to Treg instability and Foxp3 loss.

RelA deficiency leads to a defect of effector Tregs at steady state

Foxp3^{Cre} *Rela*^{lox} mice developed systemic inflammation, which in return impacted on Treg biology. Thus, to assess the intrinsic role of RelA in Tregs at steady state, we generated *Foxp3*$^{Cre/wt}$ *Rela*^{lox} heterozygous females, in which theoretically half of Tregs expressed RelA and the other half were RelA-deficient because of the localization of *Foxp3* locus in the X chromosome. We observed that these mice did not have any sign of disease and inflammation, as first noticed by macroscopic observations and the absence of cell infiltration in tissues (Fig. 4A, B), which was most likely due to the presence of functional RelA-sufficient Tregs. This was further confirmed by analyzing the numbers of CD45^{+} leukocytes and Tregs that were similar in *Foxp3*$^{Cre/wt}$ *Rela*^{lox} females and *Foxp3*$^{Cre/wt}$ controls (Fig. 4C, D). Moreover, the proportions of activated conventional T cells (Tconvs), defined by the expression of CD44, CD62L and Ki67, was identical between the two mouse types (Fig. 4E). Finally, no increased level of anti-DNA auto-antibodies were detected in the serum of the *Foxp3*$^{Cre/wt}$ *Rela*^{lox} females (Fig. 4F). Thus, *Foxp3*$^{Cre/wt}$ *Rela*^{lox} heterozygous females represent a proper model to study the intrinsic role of RelA in Tregs.

In the *Foxp3*$^{Cre/wt}$ control females, CRE-expressing Tregs (CRE^{+}) were present in lower proportion compared to Tregs not expressing CRE (CRE^{-}) (Fig. 5A, grey bars). The same tendency was observed for the different molecules that we investigated (Fig. 5B-E, grey bars), suggesting that the CRE transgene impacts on Treg biology in this competitive condition.

Compared to these controls, the knockout of RelA did not modify significantly the proportion of Tregs (Fig. 5A, green bars) nor the proportion of Tregs expressing ICOS, CTLA-4, Nrp1 or Helios (Sup. Fig. 6). However, the absence of RelA expression had a severe impact on Treg activation since the proportions of $CD44^{high}CD62L^{low}$, $Ki67^{+}$, $CD103^{+}$ and the expression level of GITR among CRE^{+} Tregs were strongly and systematically reduced (Fig. 5B-E). In conclusion, RelA expression by Tregs appears critical for the acquisition of their effector phenotype at the steady state.

RelA plays an important role in Treg activation

To characterize more extensively the effects of the RelA deficiency on Tregs, we purified CRE-expressing Tregs from *Foxp3*$^{Cre/wt}$ (WT) and *Foxp3*$^{Cre/wt}$ *Rela*^{lox} (RelA KO) mice and profiled their transcriptomes by low-input RNAseq. Overall, transcriptome differences were modest (Fig. 6A, B), with 180 differentially expressed genes at an arbitrary fold change cutoff of 2.0 (and false discovery rate <0.05). The most biased transcript was *Klrg1*, as previously reported (Messina et al. 2016), but several other transcripts involved in Treg function and/or homing in the gut and skin showed a significant bias (*e.g. Ccr4, Ccr6, Maf*, *Ahr and Itgae*). (Fig. 6B, C). Gene ontology analysis did not reveal any evocative common pathway, so we projected various Treg-specific signatures onto the comparison of WT vs. RelA KO Tregs profiles (Fig. 6D). RelA deficit modestly but significantly affected Treg identity as it reduced the canonical signature of genes differentially expressed in Tregs compared to Tconv cells (Hill et al. 2007) (Fig. 6D, left). Moreover, consistent with the phenotype described above showing reduced proportion of activation markers in RelA-deficient Tregs in *Foxp3*$^{Cre/wt}$ *Rela*^{lox} mice, a stronger bias was observed for signatures typical of activated Tregs (from comparison of $CD44^{hi}$ vs $CD62L^{hi}$ Tregs, or from Blimp1- WT vs KO Tregs (Cretney et al. 2011)). Indeed, RelA-deficient Tregs had a transcriptional signature analogous to $CD62L^{hi}$ Tregs and Blimp1 KO

Tregs, corresponding to resting-like Tregs (Fig. 6D, middle and right). This effect was not unique to activated Treg signature, as GSEA analysis showed a strong bias of generic signatures of activated $CD4^+$ or $CD8^+$ Tconv cells (Kaech et al. 2002) (Fig. 6E). For further resolution, we cross-matched the RelA WT/KO difference to a curated series of 289 signatures that distinguish different sub-phenotypes of Tregs (Zemmour et al. 2018) (Fig. 6F). The enrichment score of several gene sets characterizing activated or effector Tregs were decreased in RelA KO Tregs compared to WT Tregs (lower region of Fig. 6F). Interestingly, however, RelA-deficient Tregs were enriched in several signatures resulting from the expression of TF with inhibitory roles in Tregs, and most markedly for Bach2 (upper region of Fig. 6F). Indeed, the changes found here in response to RelA deficiency were largely anti-correlated with changes provoked by the absence of Bach2 in a previous report (Roychoudhuri et al. 2013) (Fig. 6G, $r = -0.13$ with $p<10^{-15}$ using a Pearson correlation). Overall, compared to WT Tregs, the transcriptomic signature of RelA-deficient Tregs confirmed their resting phenotype.

RelA-deficient Tregs have a defect of stability

Our RNAseq data indicate an identity defect of RelA-deficient Tregs, which was first suggested in the colitis model (Fig. 3E-G). However, one cannot conclude from this latter experiment that RelA plays an intrinsic role in Treg stability, owing to the very severe colitis developed by the mice injected with RelA-deficient Tregs. Indeed, increased instability of these latter could be well due to increased inflammation, and not RelA deficiency, since it is well established that different inflammatory factors precipitate Foxp3 loss (Zhou et al. 2009). Thus, we further investigated whether RelA had any role in maintenance of Treg stability and identity by analyzing Foxp3 expression after co-transfer of RelA-sufficient and -deficient Tregs into the same mouse. Cells were purified from *Foxp3*$^{Cre/wt}$ *Rela*^{lox} mice (*Foxp3*$^{Cre/wt}$ for controls) and not from *Foxp3*^{Cre} *Rela*^{lox} mice, since systemic inflammation in these latter mice could modify

Treg biology in addition to the impact of the RelA defect. Tregs were co-transfered in CD3 KO mice with Tconvs to sustain viability and expansion of injected Tregs (Fig. 7A). Sixteen days after transfer, the proportions of RelA-deficient cells were much lower than the ones of RelA-sufficient cells (Fig. 7B), particularly in the colon, a location subjected to high inflammation in this setting. Importantly, a large fraction of RelA-deficient Tregs lost Foxp3 expression, becoming so-called ex-Tregs, in all lymphoid and non-lymphoid tissues, compared to RelA-sufficient Tregs (Fig. 7C). Moreover, RelA-deficient ex-Tregs expressed higher amounts of the pro-inflammatory cytokines IFNγ and TNFα, in the spleen and mLN, than their wildtype counterparts (Fig. 7D).

To further explore the mechanism of Treg instability, and since it has been reported that c-Rel is involved in the differentiation of Th1 and Th17 cells (Hilliard et al. 2002; Ruan et al. 2011), we performed electrophoretic mobility shift assays (EMSA) combined with supershifts to assess the activation status of the different NF-κB subunits in Tregs of *Foxp3*^{Cre} and *Foxp3*^{Cre} *Rela*^{lox} mice (Fig. 7E). In control Tregs, there was mainly an activation of RelA, rather than RelB or c-Rel. As expected, we did not observe this phenomenon in RelA-deficient Tregs, confirming that the truncated RelA protein was not functional. However, in Tregs of *Foxp3*^{Cre} *Rela*^{lox} mice there were much more activated NF-κB complexes, obviously due to the more activated phenotype of Tregs in these mice, which were mostly, if not only, constituted of c-Rel subunit. This massive c-Rel activation may be involved in Treg instability. In conclusion, our data show that lack of RelA activation strongly affect Treg stability leading to Foxp3 loss and increased differentiation of ex-Tregs, which may turn pathogenic through the production of inflammatory cytokines.

DISCUSSION

Here, we show that RelA plays a major role in Treg biology, both at steady state and during inflammation, since its specific deletion leads to the development of a spontaneous, severe and systemic autoimmune syndrome.

The disease recapitulates some of the symptoms observed in Treg-deficient scurfy mice, although with a slower kinetics (Sakaguchi et al. 2006). As in scurfy mice, the skin and lymphoid organs are the most impaired tissues of *Foxp3*^{Cre} *Rela*^{lox}, followed by the lung, stomach and colon and at lower extent the small intestine and liver. Also, we detected DNA auto-antibodies in the serum of our mice, as in scurfy mice (Sharma et al. 2009; Hadaschik et al. 2015). We thus presume that *Foxp3*^{Cre} *Rela*^{lox} mice develop an autoimmune syndrome due to defective Tregs. Importantly, modification of the microbiota could play a major role in some tissue impairment such as the colon. Indeed, in *Foxp3*-deficient mice, colon damage becomes severe only after weaning, when microbial flora develops extensively (Sharma et al. 2009). Our data suggest that this disease is initially due to a major activation defect of RelA-deficient Tregs. Indeed, in the *Foxp3*$^{Cre/wt}$ *Rela*^{lox} non-inflamed mice, we observed reduced numbers of effector Tregs and suppressive molecules among the RelA-deficient Tregs. We thus speculate that in the *Foxp3*^{Cre} *Rela*^{lox} mice, and more specifically in tissues that are in contact with external environment and microbiota like the intestine and skin, effector T cells and myeloid cells become highly activated because of insufficient control by effector Tregs. Moreover, the decreased Treg proportion and number observed in those tissues in 5 week-old *Foxp3*^{Cre} *Rela*^{lox}, potentially due to Treg instability and a decreased expression of gut and skin homing molecules (reduced mRNA levels of *Ccr4*, *Ccr6*) (Sather et al. 2007; Kitamura, Farber, et Kelsall 2010), may exacerbate this phenomenon. Then, inflammatory factors may alter drastically stability of RelA-deficient Tregs most of them becoming pathogenic ex-Tregs, as we observed in the colitis

287 model and cell co-transfer in lymphopenic mice experiments, precipitating local inflammation.
288 The combination of reduced Treg number in the intestine and the skin, reduced Treg activation
289 and the generation of pathogenic ex-Tregs may be the driving forces of the autoimmune
290 syndrome of *Foxp3*^{Cre} *Rela*^{lox} mice.
291
292 Recent reports describe similar conditional KO mice developing a related autoimmune
293 syndrome (Messina et al. 2016; Vasanthakumar et al. 2017; Oh et al. 2017). They observed that
294 *Foxp3*^{Cre} *Rela*^{lox} mice developed inflammation of the skin, stomach, lung and colon, massive
295 activation of effector T cells and myeloid cells in lymphoid organs and high levels of
296 inflammatory cytokines, immunoglobulins and anti-DNA in the serum. We confirmed these
297 data and got deeper into the analysis of the disease since we showed that the effector T cells
298 and myeloid cells were also drastically activated in multiple non-lymphoid organs. These data
299 suggest a major defect of RelA-deficient Tregs. In addition, the injection of WT Tregs before
300 7 days of age was sufficient to stop the development of the pathology (data not shown).
301 Surprisingly, we and others observed an increase of Treg proportion in lymphoid organs and *in*
302 *vitro* assays did not reveal Treg suppressive defect. However, our extensive analysis enabled to
303 point out a decrease of Treg proportion in the inflamed non-lymphoid tissues, such as the colon
304 and skin. Our RNAseq analysis revealed a decreased expression of *Ccr4, Ccr6, Maf, Ahr* and
305 *Itgae* (encoding for CD103) which are involved in Treg function and/or homing in those tissues.
306 Particularly, it has been shown that *Ahr* regulates the expression of *Ccr6* and *Itgae* and that *Ahr*
307 deletion in Tregs leads to their decrease in the gut (Ye et al. 2017). As discussed above, this
308 initial event may ignite the whole immune system, leading to widespread activation of the
309 lymphoid and myeloid compartments and release of inflammatory cytokines that will boost
310 global Treg activation and expansion, which remains insufficient to control the pathology.
311

312 Investigating initial events that led to disease could not be properly analyzed in *Foxp3*^{Cre} *Rela*^{lox}
313 mice since inflammation has major impact on Treg migration, survival, activation, suppressive
314 function or stability (Zhou et al. 2009; van der Veeken et al. 2016), confounding the
315 interpretation of what was due to inflammation or to the intrinsic RelA deficit. Using *Lck*^{Cre}
316 *Rela*^{lox} mice, Messina *et al.* suggested that a major alteration of RelA-deficient Tregs was their
317 defect to differentiate in effector Tregs (Messina et al. 2016). However, in this work, this defect
318 was only partial, observed in LN and not in the spleen, and mostly analyzed in a quite irrelevant
319 model since RelA was knockout in whole T cells. Vasanthakumar *et al.* showed a more global
320 activation defect of RelA-deficient Tregs using *Foxp3*$^{Cre/wt}$ *Rela*^{lox} mice or mixed bone marrow
321 chimeric mice (Vasanthakumar et al. 2017). We confirmed and completed these results by
322 showing a downregulation of CD44, CD103, Ki67 and GITR not only in the lymphoid organs
323 but also in the liver and lung of *Foxp3*$^{Cre/wt}$ *Rela*^{lox} mice. Moreover, our transcriptomic analysis
324 highlighted the major activation defect of RelA-deficient Tregs, since a strong bias was
325 observed for signatures typical of activated Tregs. This reduced capacity of RelA-deficient
326 Tregs to acquire an activation status could be due to an alteration of the proper function of the
327 multimolecular complex normally containing Foxp3, p300, Helios, RelA and other TFs acting
328 as transcriptional activator (Kwon et al. 2017).
329
330 What was more consistent and unexpected was the increased instability of RelA-deficient
331 Tregs. This was first suggested in the colitis model, but more direct evidence came from studies
332 where we compared RelA-sufficient and -deficient Tregs in the same environment after cell co-
333 transfer in lymphopenic mice. We clearly showed that most RelA-deficient Tregs became ex-
334 Tregs, contrary to control Tregs. Although with reduced intensity, increased instability of Rela-
335 deficient Tregs was also observed in the absence of inflammation, as measured after transfer in
336 lymphoreplete mice (data not shown). Moreover, we detected low amounts of the truncated

RelA protein in the Tconvs of *Foxp3*^{Cre} *Rela*^{lox} mice, which may reveal the existence of ex-Tregs in these mice. Furthermore, we showed that these newly RelA-deficient ex-Tregs expressed inflammatory cytokines, suggesting that they could become pathogenic. This phenomenon may explain the increased severity observed in the colitis experiment and support our hypothesis that this ex-Tregs contribute to the pathology of *Foxp3*^{Cre} *Rela*^{lox} mice.

Foxp3 stability is controlled by histone and protein acetylation and by DNA methylation in the CNS 2 of *Foxp3* (Polansky et al. 2008). RelA activity may impact on these epigenetic modulations by different ways. RelA interacts with CBP and p300 histone/protein acetyltransferases, which seems to be critical for the recruitment of CBP and p300 to their target promoter sites, as shown in fibroblasts (Mukherjee et al. 2013). Because CBP and p300 promote *Foxp3* transcription, *Foxp3* stability at the level of CNS2 and prevent Foxp3 degradation (Liu et al. 2014; van Loosdregt et Coffer 2014), RelA-deficient Tregs may have major instability. It has also been recently reported that RelA binds to genes involved in histone modification (Vasanthakumar et al. 2017). Also, Foxp3 and RelA seem to cooperate to promote Foxp3 and CD25 expression by binding to their regulatory sequences (Soligo et al. 2011; Camperio et al. 2012), which may favor Treg stability given the known role of IL-2 receptor signaling pathway in maintenance of Treg identity (Feng et al. 2014). Furthermore, Oh *et al.* recently reported that Foxp3 expression was down-regulated in Tregs of *Foxp3*^{Cre} *cRel*^{lox} mice and even more in the *Foxp3*^{Cre} *cRel*^{lox} *RelA*^{lox} mice, suggesting that RelA favors Foxp3 expression (Oh et al. 2017). Interestingly, we observed a dramatic increased binding of c-Rel to its target DNA sequence in Tregs of *Foxp3*^{Cre} *Rela*^{lox} mice. This phenomenon may hide the genuine role of RelA in Tregs and may further increase their conversion in pathogenic cells since c-Rel has been reported to be involved in Th1 and Th17 differentiation (Hilliard et al. 2002; Ruan et al. 2011).

Overall, our study further confirms the non-redundant role of RelA in Treg biology and reveals its new role in Treg stability. There are drugs targeting NF-κB subunits. Thus, it would be of

362 strong interest to be able to target RelA in Tregs to propose new therapies triggering or
363 inhibiting Tregs in autoimmune diseases or cancer, respectively. However, RelA has an
364 important role in development and function of other immune cells (Vallabhapurapu et Karin
365 2009; Gerondakis et Siebenlist 2010; Hayden et Ghosh 2011). For instance, RelA is critical for
366 $CD4^+$ Tconv activation since its deletion prevent the development of autoimmunity in
367 *Foxp3*^{Cre} *Rela*^{lox} mice (Messina et al. 2016). Also, RelA is essential for differentiation and
368 function of Th1, Th2, Th17 and Th9 cells (Li-Weber et al. 2004; Balasubramani et al. 2010;
369 Ruan et al. 2011). Therefore, a specific targeting of RelA in Tregs would be required.

EXPERIMENTAL PROCEDURES

Mice. *Foxp3-CRE-IRES-YFP* (*Foxp3^{Cre}*) (Rubtsov et al. 2008), *RelA^{flox}* (Algül et al. 2007) and *Foxp3-IRES-GFP* (Wang et al. 2008) knock-in (*Foxp3^{GFP}*) mice were kindly given by Prs. Alexander Rudensky, Falk Weih and Bernard Malissen, respectively. *CD3e^{tm1Mal}* (*CD3$^{-/-}$*), *CD45.1*, *CD90.1* and *RAG2$^{-/-}$* mice were obtained from the cryopreservation distribution typing and animal archiving department (Orléans, France). All mice were on a C57Bl/6 background. Mice were housed under specific pathogen-free conditions. All experimental protocols were approved by the local ethics committee "Comité d'éthique en expérimentation animal Charles Darwin N°5" under the number 02811.03 and are in compliance with European Union guidelines..

Western blot. Cells were lysed for 20 min on ice in extraction buffer (0.4 M NaCl, 25 mM Hepes pH 7.7, 1.5 mM MgCl2, 0.2 mM EDTA, 1%, NP4O, 20 mM glycerol phosphate, 0.2 mM Na3VO4, 10 mM PNPP, 2mM DTT, 0.1 M PMSF). Whole cell extract was harvested after centrifuging the lysate for 10 min at 9500 X g. 20 µg of whole cell extract were separated on 7.5% SDS–polyacrylamide gels and transferred to nitrocellulose membranes (GE Healthcare). Immunoblotting was performed with anti-RelA (C20) polyclonal antibodies (Santa Cruz Biotechnology) and anti-β-actin antibody (Sigma Aldrich) and visualized using the ECL Western blotting detection kit (Pierce).

Histology. Organs were collected and fixed in PBS containing 4% formaldehyde for 48 hours and then transferred in 70% ethanol. Five-micrometer paraffin-embedded sections were cut and stained with hematoxylin and eosin and then blindly analyzed.

Cell preparation from tissues. For lymphoid tissues, cells were isolated by mechanical dilacerations. For non-lymphoid tissues, anesthetized mice were perfused intracardially with cold PBS. Small pieces of livers and lungs were digested in type IV collagenase (0.3 mg/ml) and DNase I (100 µg/ml) for 30 min at 37°C, followed by Percoll gradient (30–70%) separation. Small pieces of intestines, removed of their Peyer patches and epithelium, were digested in type IV collagenase (1 mg/ml) and DNase I (10 µg/ml) for 30 min at 37°C, followed by Percoll gradient (40–80%) separation. Small pieces of skin were digested in liberase DL (0.4mg/ml), collagenase D (0.05 mg/ml) and DNase I (10µg/ml) for 1h at 37°C, followed by Percoll gradient (40–80%) separation.

Antibodies and flow cytometry analysis. The following mAbs from BD Biosciences were used: anti-CD45 (30-F11), anti-CD8 (53-6.7), anti-CD4 (RM4-5), anti-CD62L (MEL-14), anti-CD90.1 (OX-7), anti-CD45.1 (A20), anti-CD45.2 (104), anti-CD25 (PC61 or 7D4), anti-ICOS (7E.17G9), anti-GITR (DTA-1), anti-CD103 (M290), anti-Helios (22F6), anti-CTLA-4 (UC10-4F10-11), anti-CD11b (M1/70), anti-CD11c (HL3), anti-CD19 (1D3), anti-IA/E (M5/114.15.2), anti-Ly6C (AL-21), anti-Ly6G (1A8). Anti-GFP antibody was purchased from Life Technologies. Anti-CD3 (145-2C11), anti-Foxp3 (FJK-16s), anti-CD44 (IM7), anti-Ki-67 (SOLA15), anti-Nrp1 (3DS304M), anti-NKp46 (29A1.4) and anti-F4/80 (BM8) were purchased from eBioscience, and Foxp3 staining was performed using the eBioscience kit and protocol. Cells were acquired on a BD LSRII and a BD Fortessa X20 cytometers and analyzed using FlowJo software.

Cytokine quantification. Serum cytokines were quantified using the mouse Th1/Th2/Th17 Cytokine CBA Kit (BD Biosciences) according to manufacturer's procedure. Datas were analyzed using FCAP array software.

Immunoglobulin and autoantibody quantification by ELISA. 96-well flat plates were coated with either salmon sperm DNA (Sigma) or with goat anti-mouse IgM, IgA, IgE, IgG1, IgG2b (Southern Biotech). After washes, they were saturated with BSA and first incubated with mice sera, then with biotinylated goat anti-mouse IgG (Southern Biotech) or goat anti-mouse IgM, IgA, IgE, IgG1, IgG2b (Southern Biotech). A streptavidin-horseradish conjugate (Sigma) was added followed by the addition of TMB (eBioscience). The reaction was stopped with HCl (1N) and revealed with an ELISA plate reader DTX880 Multimode Detector (Beckman Coulter).

Treg and Tconv cell purification. Treg were purified after enrichment of $CD25^+$ cells using biotinylated anti-CD25 mAb (7D4) and anti-biotin microbeads (Miltenyi Biotec), followed by CD4 staining (RM4.5) and cell sorting of $CD4^+$ Foxp3/YFP^+ cells or CD4+ Foxp3/GFP^+ using the BD FACSAria II. Tconv cells were purified after enrichment of $CD25^-$ cells using biotinylated anti-CD25 mAb (7D4) or of $CD8^-CD19^-CD11b^-$ cells using biotinylated anti-CD8 (53-6.7), CD19 (1D3) and CD11b (M1/70) mAbs and anti-biotin microbeads (Miltenyi Biotec), followed by CD4 staining (RM4.5) and cell sorting of $CD4^+$ Foxp3/YFP^- cells or CD4+ Foxp3/GFP^- using the BD FACSAria II.

Cell cultures. Purified Treg ($CD4^+YFP^+$, 25 x 10^3 cells/well) were cultured with or without whole splenocyte from CD3KO mice (7.5 x 10^4 cells/well), anti-CD3 mAb (0,05µg/ml, BioXcell), TNF (50ng/ml, Protein Service Facility, VIB, Belgium) and IL-2 (10ng/ml, Peproteck) in a 96-well round plate in RPMI 1640 10% FCS. For suppression assays, after labeling with CellTrace Violet Proliferation Kit (Life technologies), Tconv cells ($CD4^+YFP^-$, 2.5 x 10^4 cells/well) were co-cultures with various Treg ($CD4^+YFP^+$) numbers and stimulated

by splenocytes from CD3 KO mice (7.5 x 10^4 cells/well) and soluble anti-CD3 (0.05µg/ml 2C11, BioXCell) in RPMI 1640-10% FCS.

Colitis. Tconv cells ($CD4^+GFP^-$, 1 x 10^5 cells) and Tregs ($CD4^+YFP^+$, 2 x 10^4 cells) were injected intravenously into sex-matched $RAG2^{-/-}$ mice. The clinical evaluation was performed three times a week by measuring body weight. Colitis was scored on tissue sections as described previously (Martin et al. 2013).

T-cell adoptive transfer. CD3 KO mice were co-transferred with Treg ($CD4^+YFP^+$, 1 x 10^5 each) purified from age and sex-matched CD45.1/2 *Foxp3*$^{Cre/+}$ and CD45.2/2 *Foxp3*$^{Cre/+}$ *Rela*^{lox} mice and Tconv cells ($CD4^+GFP^-$, 8 x 10^5) purified from CD90.1 *Foxp3*^{GFP} mice.

Electrophoretic Mobility Shift Assays (EMSA) combined with supershit assays. Nuclear extracts were prepared and analyzed for DNA binding activity using the HIV-LTR tandem κB oligonucleotide as κB probe (Jacque et al. 2013). For supershift assays, nuclear extracts were incubated with specific antibodies for 30 min on ice before incubation with the labeled probe.

Gene-Expression Profiling and Analysis. Tregs (1,000) were double-sorted into TRIzol (Invitrogen). Subsequent sample processing was followed by Ultra-low input RNAseq protocol as described (Zemmour et al. 2017). Normalized data were analyzed with Multiplot Studio, GSEA and Gene-e modules in Genepattern. For signature enrichment analysis, each signature was curated from published datasets and computed by comparison between two conditions (e.g. WT vs KO). Data were downloaded from GEO and only the ones containing replicates were used. To reduce noise, genes with a coefficient of variation between biological replicates > 0.6 in either comparison groups were selected. Up- and down-regulated transcripts were defined as

having a fold change in gene expression > 1.5 or < 2/3 and a t.test p-value < 0.05. A signature score for each single cell was computed by summing the counts for the upregulated genes and subtracting the counts for the downregulated genes. Z scores were plotted in the heat map (Zemmour_Code/Zemmour_Code.Rmd: **Treg signatures and single cell score**).

Statistical analysis. Statistical analyses were performed using GraphPad Prism Software. Statistical significance was determined using a log-rank (Mantel- Cox) test for the mouse survival data. For all the other statistical analysis, the two-tailed unpaired nonparametric Mann–Whitney *U* test was used for data not following a normal distribution and the *t*-test was used for data following a normal distribution. *p<0.05, **p<0.01, ***p<0.001, ****p<0.0001. Means ± SEM were used throughout the figures.

AUTHOR CONTRIBUTIONS

BLS and ER designed the research. ER performed almost all the experiments and analyzed the data. MLR, RV, JD, SG and AR helped ER on some experiments. HK and CB performed and analyzed the RNA-seq data. DC and VB performed and analyzed the western blot and EMSA. BLS and ER wrote the manuscript using comments from all authors.

ACKNOWLEGMENTS

We are grateful to Pr. Alexander Rudensky and Pr. Falk Weih for providing us the *Foxp3*^{Cre} and *Rela*^{lox} mice, respectively, and Christelle Enond, Doriane Foret, Flora Issert, Olivier Bregerie, Bocar Kane and Maria Mihoc for their expert care of the mouse colony. We also want to thank Fatiha Bouhidel for helping for the histological analysis. Part of the data presented in this manuscript have been described in the PhD thesis of Emilie Ronin that is freely available online (https://tel.archives-ouvertes.fr/tel-01884171). This work was supported by the Agence Nationale de la Recherche (grant ANR-15-CE15-0015-03), the Fondation pour la Recherche Médicale (Equipes FRM 2015; FDT20160435696) and the Fondation Bettencourt Schueller.

COMPETING FINANCIAL INTERESTS.

The authors declare no competing financial interests.

REFERENCES

Algül, Hana, Matthias Treiber, Marina Lesina, Hassan Nakhai, Dieter Saur, Fabian Geisler, Alexander Pfeifer, Stephan Paxian, et Roland M. Schmid. 2007. « Pancreas-Specific RelA/P65 Truncation Increases Susceptibility of Acini to Inflammation-Associated Cell Death Following Cerulein Pancreatitis ». *The Journal of Clinical Investigation* 117 (6): 1490-1501. https://doi.org/10.1172/JCI29882.

Bettelli, Estelle, Maryam Dastrange, et Mohamed Oukka. 2005. « Foxp3 Interacts with Nuclear Factor of Activated T Cells and NF-KB to Repress Cytokine Gene Expression and Effector Functions of T Helper Cells ». *Proceedings of the National Academy of Sciences of the United States of America* 102 (14): 5138-43. https://doi.org/10.1073/pnas.0501675102.

Camperio, Cristina, Silvana Caristi, Giorgia Fanelli, Marzia Soligo, Paola Del Porto, et Enza Piccolella. 2012. « Forkhead Transcription Factor FOXP3 Upregulates CD25 Expression through Cooperation with RelA/NF-κB ». *PLOS ONE* 7 (10): e48303. https://doi.org/10.1371/journal.pone.0048303.

Chang, Jae-Hoon, Yichuan Xiao, Hongbo Hu, Jin Jin, Jiayi Yu, Xiaofei Zhou, Xuefeng Wu, et al. 2012. « Ubc13 Maintains the Suppressive Function of Regulatory T Cells and Prevents Their Conversion into Effector-like T Cells ». *Nature Immunology* 13 (5): 481-90. https://doi.org/10.1038/ni.2267.

Chaudhry, Ashutosh, Dipayan Rudra, Piper Treuting, Robert M. Samstein, Yuqiong Liang, Arnold Kas, et Alexander Y. Rudensky. 2009. « $CD4^+$ Regulatory T Cells Control T_H17 Responses in a Stat3-Dependent Manner ». *Science* 326 (5955): 986-91. https://doi.org/10.1126/science.1172702.

Chen, Xin, Jami Willette-Brown, Xueqiang Wu, Ya Hu, O. M. Zack Howard, Yinling Hu, et Joost J. Oppenheim. 2015. « IKKα Is Required for the Homeostasis of Regulatory T Cells and for the Expansion of Both Regulatory and Effector CD4 T Cells ». *The FASEB Journal* 29 (2): 443-54. https://doi.org/10.1096/fj.14-259564.

Cipolletta, Daniela, Markus Feuerer, Amy Li, Nozomu Kamei, Jongsoon Lee, Steven E. Shoelson, Christophe Benoist, et Diane Mathis. 2012. « PPAR-γ Is a Major Driver of the Accumulation and Phenotype of Adipose Tissue Treg Cells ». *Nature* 486 (7404): 549-53. https://doi.org/10.1038/nature11132.

Cretney, Erika, Annie Xin, Wei Shi, Martina Minnich, Frederick Masson, Maria Miasari, Gabrielle T. Belz, et al. 2011. « The Transcription Factors Blimp-1 and IRF4 Jointly Control the Differentiation and Function of Effector Regulatory T Cells ». *Nature Immunology* 12 (4): 304-11. https://doi.org/10.1038/ni.2006.

Dias, Sheila, Angela D'Amico, Erika Cretney, Yang Liao, Julie Tellier, Christine Bruggeman, Francisca F. Almeida, et al. 2017. « Effector Regulatory T Cell Differentiation and Immune Homeostasis Depend on the Transcription Factor Myb ». *Immunity* 46 (1): 78-91. https://doi.org/10.1016/j.immuni.2016.12.017.

DuPage, Michel, Gaurav Chopra, Jason Quiros, Wendy L. Rosenthal, Malika M. Morar, Dan Holohan, Ruan Zhang, Laurence Turka, Alexander Marson, et Jeffrey A. Bluestone. 2015. « The Chromatin-Modifying Enzyme Ezh2 Is Critical for the Maintenance of Regulatory T Cell Identity after Activation ». *Immunity* 42 (2): 227-38. https://doi.org/10.1016/j.immuni.2015.01.007.

Feng, Yongqiang, Aaron Arvey, Takatoshi Chinen, Joris van der Veeken, Georg Gasteiger, et Alexander Y. Rudensky. 2014. « Control of the Inheritance of Regulatory T Cell Identity by a

cis Element in the Foxp3 Locus ». *Cell* 158 (4): 749-63. https://doi.org/10.1016/j.cell.2014.07.031.

Garg, Garima, Andreas Muschaweckh, Helena Moreno, Ajithkumar Vasanthakumar, Stefan Floess, Gildas Lepennetier, Rupert Oellinger, et al. 2019. « Blimp1 Prevents Methylation of Foxp3 and Loss of Regulatory T Cell Identity at Sites of Inflammation ». *Cell Reports* 26 (7): 1854-1868.e5. https://doi.org/10.1016/j.celrep.2019.01.070.

Hadaschik, Eva N., Xiaoying Wei, Harald Leiss, Britta Heckmann, Birgit Niederreiter, Günter Steiner, Walter Ulrich, Alexander H. Enk, Josef S. Smolen, et Georg H. Stummvoll. 2015. « Regulatory T cell-deficient scurfy mice develop systemic autoimmune features resembling lupus-like disease ». *Arthritis Research & Therapy* 17 (1): 35. https://doi.org/10.1186/s13075-015-0538-0.

Heuser, Christoph, Janine Gotot, Eveline Christina Piotrowski, Marie-Sophie Philipp, Christina Johanna Felicia Courrèges, Martin Sylvester Otte, Linlin Guo, et al. 2017. « Prolonged IKKβ Inhibition Improves Ongoing CTL Antitumor Responses by Incapacitating Regulatory T Cells ». *Cell Reports* 21 (3): 578-86. https://doi.org/10.1016/j.celrep.2017.09.082.

Hill, Jonathan A., Markus Feuerer, Kaley Tash, Sokol Haxhinasto, Jasmine Perez, Rachel Melamed, Diane Mathis, et Christophe Benoist. 2007. « Foxp3 Transcription-Factor-Dependent and -Independent Regulation of the Regulatory T Cell Transcriptional Signature ». *Immunity* 27 (5): 786-800. https://doi.org/10.1016/j.immuni.2007.09.010.

Hilliard, Brendan A., Nicola Mason, Lingyun Xu, Jing Sun, Salah-Eddine Lamhamedi-Cherradi, Hsiou-Chi Liou, Christopher Hunter, et Youhai H. Chen. 2002. « Critical Roles of C-Rel in Autoimmune Inflammation and Helper T Cell Differentiation ». *The Journal of Clinical Investigation* 110 (6): 843-50. https://doi.org/10.1172/JCI15254.

Isomura, Iwao, Stephanie Palmer, Raelene J. Grumont, Karen Bunting, Gerard Hoyne, Nancy Wilkinson, Ashish Banerjee, et al. 2009. « C-Rel Is Required for the Development of Thymic Foxp3+ CD4 Regulatory T Cells ». *Journal of Experimental Medicine* 206 (13): 3001-14. https://doi.org/10.1084/jem.20091411.

Jacque, E., K. Billot, H. Authier, D. Bordereaux, et V. Baud. 2013. « RelB Inhibits Cell Proliferation and Tumor Growth through P53 Transcriptional Activation ». *Oncogene* 32 (21): 2661-69. https://doi.org/10.1038/onc.2012.282.

Kaech, Susan M., Scott Hemby, Ellen Kersh, et Rafi Ahmed. 2002. « Molecular and Functional Profiling of Memory CD8 T Cell Differentiation ». *Cell* 111 (6): 837-51. https://doi.org/10.1016/S0092-8674(02)01139-X.

Kitamura, Kazuya, Joshua M. Farber, et Brian L. Kelsall. 2010. « CCR6 marks regulatory T cells as a colon-tropic, interleukin-10-producing phenotype ». *Journal of immunology (Baltimore, Md. : 1950)* 185 (6): 3295-3304. https://doi.org/10.4049/jimmunol.1001156.

Koch, Meghan A., Glady's Tucker-Heard, Nikole R. Perdue, Justin R. Killebrew, Kevin B. Urdahl, et Daniel J. Campbell. 2009. « The Transcription Factor T-Bet Controls Regulatory T Cell Homeostasis and Function during Type 1 Inflammation ». *Nature Immunology* 10 (6): 595-602. https://doi.org/10.1038/ni.1731.

Kwon, Ho-Keun, Hui-Min Chen, Diane Mathis, et Christophe Benoist. 2017. « Different Molecular Complexes That Mediate Transcriptional Induction and Repression by FoxP3 ». *Nature Immunology* 18 (11): ni.3835. https://doi.org/10.1038/ni.3835.

Linterman, Michelle A., Wim Pierson, Sau K. Lee, Axel Kallies, Shimpei Kawamoto, Tim F. Rayner, Monika Srivastava, et al. 2011. « Foxp3+ Follicular Regulatory T Cells Control the

596 Germinal Center Response ». *Nature Medicine* 17 (8): 975-82.
597 https://doi.org/10.1038/nm.2425.

598 Liu, Yujie, Liqing Wang, Rongxiang Han, Ulf H. Beier, Tatiana Akimova, Tricia Bhatti,
599 Haiyan Xiao, Philip A. Cole, Paul K. Brindle, et Wayne W. Hancock. 2014. « Two
600 Histone/Protein Acetyltransferases, CBP and P300, Are Indispensable for Foxp3+ T-
601 Regulatory Cell Development and Function ». *Molecular and Cellular Biology* 34 (21):
602 3993-4007. https://doi.org/10.1128/MCB.00919-14.

603 Long, Meixiao, Sung-Gyoo Park, Ian Strickland, Matthew S. Hayden, et Sankar Ghosh. 2009.
604 « Nuclear Factor-κB Modulates Regulatory T Cell Development by Directly Regulating
605 Expression of Foxp3 Transcription Factor ». *Immunity* 31 (6): 921-31.
606 https://doi.org/10.1016/j.immuni.2009.09.022.

607 Loosdregt, Jorg van, et Paul J. Coffer. 2014. « Post-translational modification networks
608 regulating FOXP3 function ». *Trends in Immunology* 35 (8): 368-78.
609 https://doi.org/10.1016/j.it.2014.06.005.

610 Martin, Bruno, Cédric Auffray, Arnaud Delpoux, Arnaud Pommier, Aurélie Durand, Céline
611 Charvet, Philippe Yakonowsky, et al. 2013. « Highly Self-Reactive Naive CD4 T Cells Are
612 Prone to Differentiate into Regulatory T Cells ». *Nature Communications* 4 (juillet):
613 ncomms3209. https://doi.org/10.1038/ncomms3209.

614 Messina, Nicole, Thomas Fulford, Lorraine O'Reilly, Wen Xian Loh, Jessica M. Motyer, Darcy
615 Ellis, Catriona McLean, et al. 2016. « The NF-κB transcription factor RelA is required for the
616 tolerogenic function of Foxp3+ regulatory T cells ». *Journal of Autoimmunity* 70: 52-62.
617 https://doi.org/10.1016/j.jaut.2016.03.017.

618 Mukherjee, Sulakshana P., Marcelo Behar, Harry A. Birnbaum, Alexander Hoffmann, Peter E.
619 Wright, et Gourisankar Ghosh. 2013. « Analysis of the RelA:CBP/p300 Interaction Reveals Its
620 Involvement in NF-κB-Driven Transcription ». *PLOS Biology* 11 (9): e1001647.
621 https://doi.org/10.1371/journal.pbio.1001647.

622 Oh, Hyunju, et Sankar Ghosh. 2013. « NF-KB: Roles and Regulation in Different CD4+ T-Cell
623 Subsets ». *Immunological Reviews* 252 (1): 41-51. https://doi.org/10.1111/imr.12033.

624 Oh, Hyunju, Yenkel Grinberg-Bleyer, Will Liao, Dillon Maloney, Pingzhang Wang, Zikai Wu,
625 Jiguang Wang, et al. 2017. « An NF-κB Transcription-Factor-Dependent Lineage-Specific
626 Transcriptional Program Promotes Regulatory T Cell Identity and Function ». *Immunity* 47 (3):
627 450-465.e5. https://doi.org/10.1016/j.immuni.2017.08.010.

628 Ono, Masahiro, Hiroko Yaguchi, Naganari Ohkura, Issay Kitabayashi, Yuko Nagamura,
629 Takashi Nomura, Yoshiki Miyachi, Toshihiko Tsukada, et Shimon Sakaguchi. 2007. « Foxp3
630 Controls Regulatory T-Cell Function by Interacting with AML1/Runx1 ». *Nature* 446 (7136):
631 685-89. https://doi.org/10.1038/nature05673.

632 Pan, Fan, Hong Yu, Eric V. Dang, Joseph Barbi, Xiaoyu Pan, Joseph F. Grosso, Dinili Jinasena,
633 et al. 2009. « Eos Mediates Foxp3-Dependent Gene Silencing in $CD4^+$ Regulatory T Cells ».
634 *Science* 325 (5944): 1142-46. https://doi.org/10.1126/science.1176077.

635 Polansky, Julia K., Karsten Kretschmer, Jennifer Freyer, Stefan Floess, Annette Garbe, Udo
636 Baron, Sven Olek, Alf Hamann, Harald von Boehmer, et Jochen Huehn. 2008. « DNA
637 Methylation Controls Foxp3 Gene Expression ». *European Journal of Immunology* 38 (6):
638 1654-63. https://doi.org/10.1002/eji.200838105.

639 Roychoudhuri, Rahul, Kiyoshi Hirahara, Kambiz Mousavi, David Clever, Christopher A.
640 Klebanoff, Michael Bonelli, Giuseppe Sciumè, et al. 2013. « BACH2 Represses Effector

641 Programs to Stabilize Treg-Mediated Immune Homeostasis ». *Nature* 498 (7455): 506-10.
642 https://doi.org/10.1038/nature12199.

643 Ruan, Qingguo, Vasumathi Kameswaran, Yukiko Tone, Li Li, Hsiou-Chi Liou, Mark I. Greene,
644 Masahide Tone, et Youhai H. Chen. 2009. « Development of Foxp3+ Regulatory T Cells Is
645 Driven by the C-Rel Enhanceosome ». *Immunity* 31 (6): 932-40.
646 https://doi.org/10.1016/j.immuni.2009.10.006.

647 Ruan, Qingguo, Vasumathi Kameswaran, Yan Zhang, Shijun Zheng, Jing Sun, Junmei Wang,
648 Jennifer DeVirgiliis, Hsiou-Chi Liou, Amer A. Beg, et Youhai H. Chen. 2011. « The Th17
649 Immune Response Is Controlled by the Rel–RORγ–RORγT Transcriptional Axis ». *Journal of*
650 *Experimental Medicine* 208 (11): 2321-33. https://doi.org/10.1084/jem.20110462.

651 Rubtsov, Yuri P., Jeffrey P. Rasmussen, Emil Y. Chi, Jason Fontenot, Luca Castelli, Xin Ye,
652 Piper Treuting, et al. 2008. « Regulatory T Cell-Derived Interleukin-10 Limits Inflammation at
653 Environmental Interfaces ». *Immunity* 28 (4): 546-58.
654 https://doi.org/10.1016/j.immuni.2008.02.017.

655 Sakaguchi, Shimon, Masahiro Ono, Ruka Setoguchi, Haruhiko Yagi, Shohei Hori, Zoltan
656 Fehervari, Jun Shimizu, Takeshi Takahashi, et Takashi Nomura. 2006. « Foxp3+CD25+CD4+
657 Natural Regulatory T Cells in Dominant Self-Tolerance and Autoimmune Disease ».
658 *Immunological Reviews* 212 (1): 8-27. https://doi.org/10.1111/j.0105-2896.2006.00427.x.

659 Sather, Blythe D., Piper Treuting, Nikole Perdue, Mike Miazgowicz, Jason D. Fontenot,
660 Alexander Y. Rudensky, et Daniel J. Campbell. 2007. « Altering the Distribution of Foxp3+
661 Regulatory T Cells Results in Tissue-Specific Inflammatory Disease ». *Journal of*
662 *Experimental Medicine* 204 (6): 1335-47. https://doi.org/10.1084/jem.20070081.

663 Sharma, Rahul, Sun-sang Joe Sung, Shu Man Fu, et Shyr-Te Ju. 2009. « Regulation of multi-
664 organ inflammation in the regulatory T cell-deficient scurfy mice ». *Journal of Biomedical*
665 *Science* 16 (1): 20. https://doi.org/10.1186/1423-0127-16-20.

666 Soligo, Marzia, Cristina Camperio, Silvana Caristi, Cristiano Scottà, Paola Del Porto, Antonio
667 Costanzo, Pierre-Yves Mantel, Carsten B. Schmidt-Weber, et Enza Piccolella. 2011. « CD28
668 Costimulation Regulates FOXP3 in a RelA/NF-KB-Dependent Mechanism ». *European*
669 *Journal of Immunology* 41 (2): 503-13. https://doi.org/10.1002/eji.201040712.

670 van der Veeken, Joris, Alvaro J. Gonzalez, Hyunwoo Cho, Aaron Arvey, Saskia Hemmers,
671 Christina S. Leslie, et Alexander Y. Rudensky. 2016. « Memory of Inflammation in Regulatory
672 T Cells ». *Cell* 166 (4): 977-90. https://doi.org/10.1016/j.cell.2016.07.006.

673 Vasanthakumar, Ajithkumar, Yang Liao, Peggy Teh, Maria F. Pascutti, Anna E. Oja, Alexandra
674 L. Garnham, Renee Gloury, et al. 2017. « The TNF Receptor Superfamily-NF-κB Axis Is
675 Critical to Maintain Effector Regulatory T Cells in Lymphoid and Non-lymphoid Tissues ».
676 *Cell Reports* 20 (12): 2906-20. https://doi.org/10.1016/j.celrep.2017.08.068.

677 Wang, Ying, Adrien Kissenpfennig, Michael Mingueneau, Sylvie Richelme, Pierre Perrin,
678 Stéphane Chevrier, Céline Genton, et al. 2008. « Th2 Lymphoproliferative Disorder of *Lat*^{Y136F}
679 Mutant Mice Unfolds Independently of TCR-MHC Engagement and Is Insensitive to the Action
680 of Foxp3^{+} Regulatory T Cells ». *The Journal of Immunology* 180 (3): 1565-75.
681 https://doi.org/10.4049/jimmunol.180.3.1565.

682 Wohlfert, Elizabeth A., John R. Grainger, Nicolas Bouladoux, Joanne E. Konkel, Guillaume
683 Oldenhove, Carolina Hager Ribeiro, Jason A. Hall, et al. 2011. « GATA3 Controls Foxp3^{+}
684 Regulatory T Cell Fate during Inflammation in Mice ». *The Journal of Clinical Investigation*
685 121 (11): 4503-15. https://doi.org/10.1172/JCI57456.

686 Wu, Yongqing, Madhuri Borde, Vigo Heissmeyer, Markus Feuerer, Ariya D. Lapan, James C.
687 Stroud, Darren L. Bates, et al. 2006. « FOXP3 Controls Regulatory T Cell Function through
688 Cooperation with NFAT ». *Cell* 126 (2): 375-87. https://doi.org/10.1016/j.cell.2006.05.042.

689 Yang, Ruili, Cunye Qu, Yu Zhou, Joanne E. Konkel, Shihong Shi, Yi Liu, Chider Chen, et al.
690 2015. « Hydrogen Sulfide Promotes Tet1- and Tet2-Mediated Foxp3 Demethylation to Drive
691 Regulatory T Cell Differentiation and Maintain Immune Homeostasis ». *Immunity* 43 (2):
692 251-63. https://doi.org/10.1016/j.immuni.2015.07.017.

693 Ye, Jian, Ju Qiu, John W. Bostick, Aki Ueda, Hilde Schjerven, Shiyang Li, Christian Jobin,
694 Zong-ming E. Chen, et Liang Zhou. 2017. « The Aryl Hydrocarbon Receptor Preferentially
695 Marks and Promotes Gut Regulatory T Cells ». *Cell Reports* 21 (8): 2277-90.
696 https://doi.org/10.1016/j.celrep.2017.10.114.

697 Zemmour, David, Alvin Pratama, Scott M. Loughhead, Diane Mathis, et Christophe Benoist.
698 2017. « Flicr, a Long Noncoding RNA, Modulates Foxp3 Expression and Autoimmunity ».
699 *Proceedings of the National Academy of Sciences* 114 (17): E3472-80.
700 https://doi.org/10.1073/pnas.1700946114.

701 Zemmour, David, Rapolas Zilionis, Evgeny Kiner, Allon M. Klein, Diane Mathis, et Christophe
702 Benoist. 2018. « Single-Cell Gene Expression Reveals a Landscape of Regulatory T Cell
703 Phenotypes Shaped by the TCR ». *Nature Immunology* 19 (3): 291-301.
704 https://doi.org/10.1038/s41590-018-0051-0.

705 Zheng, Ye, Ashutosh Chaudhry, Arnold Kas, Paul deRoos, Jeong M. Kim, Tin-Tin Chu, Lynn
706 Corcoran, Piper Treuting, Ulf Klein, et Alexander Y. Rudensky. 2009. « Regulatory T-Cell
707 Suppressor Program Co-Opts Transcription Factor IRF4 to Control TH2 Responses ». *Nature*
708 458 (7236): 351-56. https://doi.org/10.1038/nature07674.

709 Zhou, Xuyu, Samantha L. Bailey-Bucktrout, Lukas T. Jeker, Cristina Penaranda, Marc
710 Martínez-Llordella, Meredith Ashby, Maki Nakayama, Wendy Rosenthal, et Jeffrey A.
711 Bluestone. 2009. « Instability of the Transcription Factor Foxp3 Leads to the Generation of
712 Pathogenic Memory T Cells in Vivo ». *Nature Immunology* 10 (9): 1000-1007.
713 https://doi.org/10.1038/ni.1774.
714

Figure 1. Mice with RelA deficient Tregs develop systemic inflammation. (A) Western blot analysis of RelA expression in Tregs and $CD4^+$ conventional T cells (Tconv) isolated from *Foxp3*^{Cre} (*Cre*) and *Foxp3*^{Cre} *Rela*^{lox} (*Cre Rela*^{lox}) mice. (B) Representative pictures of 12 week-old *Foxp3*^{Cre} and *Foxp3*^{Cre} *Rela*^{lox} mice. (C) Body weight monitoring of *Foxp3*^{Cre} and *Foxp3*^{Cre} *Rela*^{lox} males and females. (D) Percentages of *Foxp3*^{Cre} *Rela*^{lox} mice with skin lesions. (E) Survival monitoring of *Foxp3*^{Cre} *Rela*^{lox} mice. (F) Representative pictures from 20 mice of the LN and colon of 12 week-old *Foxp3*^{Cre} and *Foxp3*^{Cre} *Rela*^{lox} mice. (G) Weight/length ratio of colon of 12 week-old *Foxp3*^{Cre} and *Foxp3*^{Cre} *Rela*^{lox} mice. (H) Representative histology from 12 week-old mice of the lung, stomach, colon, skin and ear of *Foxp3*^{Cre} and *Foxp3*^{Cre} *Rela*^{lox}. Scale bars represent 200µm (lung, *Foxp3*^{Cre} stomach, colon), 150µm (*Foxp3*^{Cre} *Rela*^{lox} stomach) and 100µm (skin, ear). Data are representative of independent experiments. Bars show the means and error bars represent SEM. For mouse and experiment numbers, see Supplementary Table 1. Statistical significance was determined using a log-rank (Mantel- Cox) test for the mouse survival data. The two-tailed unpaired nonparametric Mann–Whitney *U* test was used. $^{**}p<0.01$, $^{***}p<0.001$.

Figure 2. High activation of T and B lymphocytes in *Foxp3*^{Cre} *Rela*^{lox} mice. (A, B) Number of $CD45^+$ (A), $CD8^+$, $CD4^+$ and B cells (B) in the indicated organs (spl=spleen, liv=liver, SI= small intestine) of 12 week-old *Foxp3*^{Cre} (*Cre*) and *Foxp3*^{Cre} *Rela*^{lox} (*Cre Rela*^{lox}) mice. (C, D) Representative dot plots and proportion of $CD44^{hi}$ $CD62L^{low}$ (C) and $Ki67^+$ (D) among $CD8^+$ and $CD4^+$ Tconv in the indicated organs of 12 week-old *Foxp3*^{Cre} and *Foxp3*^{Cre} *Rela*^{lox} mice. (E) Cytokine quantification in the serum of 4-12 week-old *Foxp3*^{Cre}, and 4-6 week-old and 9-14 week-old *Foxp3*^{Cre} *Rela*^{lox} mice. (F) Immunoglobulin quantification in the serum of 4-12 week-old *Foxp3*^{Cre} mice, and 4-6 week-old and 13 week-old *Foxp3*^{Cre} *Rela*^{lox} mice. (G) Anti-DNA antibody quantification in the serum of 4-15 week-old *Foxp3*^{Cre} mice, and 4-12 week-old

and 12-14 week-old *Foxp3*^{Cre} *Rela*^{lox} mice. Each dot represents a mouse, lines and bars show the means of pooled independent experiments. Error bars represent SEM. For mouse and experiment numbers, see Supplementary Table 1. The two-tailed unpaired nonparametric Mann–Whitney *U* test was used for data not following a normal distribution and the *t*-test was used for data following a normal distribution. *p<0.05, **p<0.01, ***p<0.001, ****p<0.0001.

Figure 3. Tregs in *Foxp3*^{Cre} *Rela*^{lox} mice appear to be less stable. (A) Representative density plot and proportion of Tregs among the CD4^{+} T cells in the indicated organs (thy= thymus, spl=spleen, liv=liver, SI= small intestine) of 12 week-old *Foxp3*^{Cre} (*Cre*) and *Foxp3*^{Cre} *Rela*^{lox} (*Cre Rela*^{lox}) mice. (B) Proportion of Tregs among CD4+ cells in 5 week-old *Foxp3*^{Cre} and *Foxp3*^{Cre} *Rela*^{lox} mice. (C) Representative density plots and proportions of CD44^{hi} CD62L^{low} among the Tregs of 12 week-old *Foxp3*^{Cre} and *Foxp3*^{Cre} *Rela*^{lox} mice. Each dot represents a mouse and lines show the means of pooled independent experiments. (D) *In vitro* suppressive activity of Treg cells from *Foxp3*^{Cre} (WT Tregs) and *Foxp3*^{Cre} *Rela*^{lox} (KO Tregs) 5-6 week-old mice. Representative data at 2:1, 1:2 and 1:8 (left) and different (right) Treg:Tconv ratios of independent experiments. (E-G) *In vivo* suppressive activity of Treg cells from *Foxp3*^{Cre} (WT Tregs, 6 week-old mice) and *Foxp3*^{Cre} *Rela*^{lox} (KO Tregs, 6 week-old mice) mice, determined in a colitis model stopped at 6 weeks for analyses. (E) Percentage of initial body weight pooled from independent experiments. Error bars represent SEM. (F) Representative histology of the colon and colitis scores. (G) Numbers of recovered Tregs (CD90.1^{-} cells), representative histograms and proportions of ex-Treg in the mLN and colon. Each dot represents a mouse and lines show the means of pooled independent experiments. For mouse and experiment numbers, see Supplementary Table 1. The two-tailed unpaired nonparametric Mann–Whitney *U* test was used for data not following a normal distribution and the *t*-test was used for data following a normal distribution. *p<0.05, **p<0.01, ***p<0.001, ****p<0.0001.

Figure 4. Heterozygous *Foxp3*$^{Cre/wt}$ *Rela*^{lox} do not develop systemic inflammation. (A) Representative pictures of 8 week-old mice. (B) Representative histology of lung, colon and skin of 8 week-old. Scale bars represent 100µm. Number of CD45$^+$ (C), of Tregs among CD4$^+$ T cells (D) and proportion of CD44^{hi}CD62L^{low} and Ki67$^+$ among CD8$^+$ and CD4$^+$ conventional T cells (E) in different tissues (thy=thymus, spl=spleen, liv=liver, SI= small intestine) of 8 week-old *Foxp3*$^{Cre/wt}$ (*Cre/wt*) and *Foxp3*$^{Cre/wt}$ *Rela*^{lox} (*Cre/wt Rela*^{lox}) mice. Each dot represents a mouse and lines show the means of pooled independent experiments. (F) Anti-DNA auto-antibodies quantification in the serum of 8 week-old *Foxp3*$^{Cre/wt}$ and *Foxp3*$^{Cre/wt}$ *Rela*^{lox} mice. Bars show the means of pooled independent experiments and error bars represent SEM. For mouse and experiment numbers, see Supplementary Table 1. The two-tailed unpaired nonparametric Mann–Whitney *U* test was used. *p<0.05.

Figure 5. Reduced expression of activation markers in RelA-deficient Tregs at steady state. Analyses in the indicated organs (thy= thymus, spl=spleen, liv=liver) of 8 week-old *Foxp3*$^{Cre/wt}$ (*Cre/wt* – grey bars) and *Foxp3*$^{Cre/wt}$ *Rela*^{lox} (*Cre/wt Rela*^{lox} – green bars) mice. (A) Representative density plots among CD4$^+$ cells to define Tregs expressing CRE (CRE$^+$) and percentages of CRE$^+$ among total Tregs in sdLN. Representative density plots and proportions of CD44^{hi} CD62L^{low} (B), Ki67$^+$ (C), CD103$^+$ (D) and MFI of GITR (E) among CRE$^+$ Tregs of sdLN. Bars show the means of pooled independent experiments and error bars represent SEM. For mouse and experiment numbers, see Supplementary Table 1. The two-tailed unpaired nonparametric Mann–Whitney *U* test was used. *p<0.05, **p<0.01, ***p<0.001.

Figure 6. RelA-deficient Tregs have identity and activation defects. (A) PCA analysis of WT and RelA KO Tregs. (B) Volcano plot of WT vs. RelA KO Tregs. Red and green indicate

790 transcripts up- and down-regulated, respectively, by WT Tregs cells. (C) Relative expression
791 of *Itgae* (CD103) expressed in counts per million in WT and RelA KO Tregs. (D) WT vs. RelA
792 KO Tregs (as in A) overlaid with various Tregs signatures. Red and green indicate genes up-
793 and down-regulated, respectively, in each signature (chi-squared test for p-value). (E) GSEA
794 plots of RelA-deficient Tregs compared with indicated set of genes up-regulated in effector
795 memory CD4 (upper panel) and memory CD8 conventional T cells (lower panel) (Kaech et al.
796 2002). (F) Heatmap for the enrichment score of each gene signature (VAT= visceral adipose
797 tissue, LN= lymph nodes, SI= small intestine, Sp= spleen). (G) Fold change-fold change plot
798 of WT vs RelA KO Tregs (x-axis) and WT iTregs vs WT Bach2 KO iTregs (y-axis, from
799 published data (Roychoudhuri et al. 2013)). Red and green transcripts from (A). For mouse and
800 experiment numbers, see Supplementary Table 1.
801
802 **Figure 7. RelA-deficient Tregs are unstable and turn pathogenic.** (A-D) Adoptive transfer
803 of a 1:1:8 ratio of a mix of CRE-expressing Tregs from *Foxp3*$^{Cre/wt}$ (CD45.1/2 CD90.2 WT
804 Tregs), *Foxp3*$^{Cre/wt}$ *Rela*^{lox} (CD45.2 CD90.2 RelA KO Tregs) mice and CD4^{+} conventional T
805 cells (CD90.1 Tconv) into CD3 KO mice and analysis of donor cells 16 days later. (A)
806 Experimental scheme and representative gating strategy from sdLN staining. (B) Ratio of RelA
807 KO to WT Tregs in the indicated organs (spl=spleen, liv=liver, SI= small intestine) among
808 CD90.2^{+} donor cells. The horizontal dot line represents the initial ratio (in the syringe). (C)
809 Representative histograms and proportion of ex-Tregs from injected WT cells and RelA KO
810 cells in different tissues. (D) Representative density plots and proportions of IFNγ^{+} and TNF^{+}
811 cells among WT ex-Tregs and RelA KO ex-Tregs. Each dot represents a mouse, lines and bars
812 show the means of pooled independent experiments. Error bars represent SEM. (E) EMSA
813 combined with supershift assay analysis of NF-κB subunits activation in Tregs isolated from
814 *Foxp3*^{Cre} (*Cre*) and *Foxp3*^{Cre} *Rela*^{lox} (*Cre Rela*^{lox}) mice. The yellow squares point out the

supershift of RelA or c-Rel containing complexes. The results are representative of independent experiments. For mouse and experiment numbers, see Supplementary Table 1. The two-tailed unpaired nonparametric Mann–Whitney *U* test was used for data not following a normal distribution and the *t*-test was used for data following a normal distribution. **p*<0.05, ***p*<0.01, ****p*<0.001, *****p*<0.0001.

Figure 01.TIFF

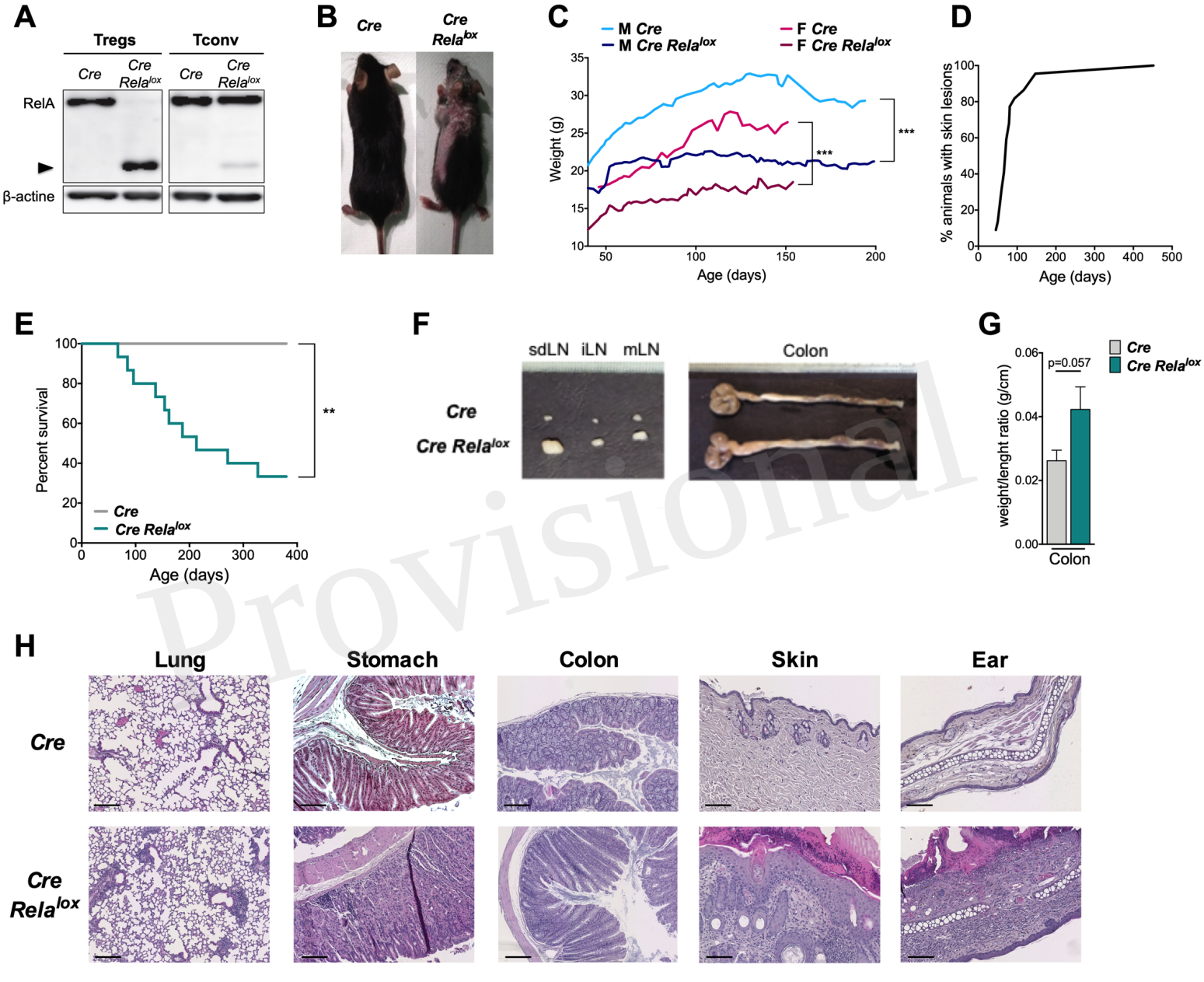

Figure 02.TIFF

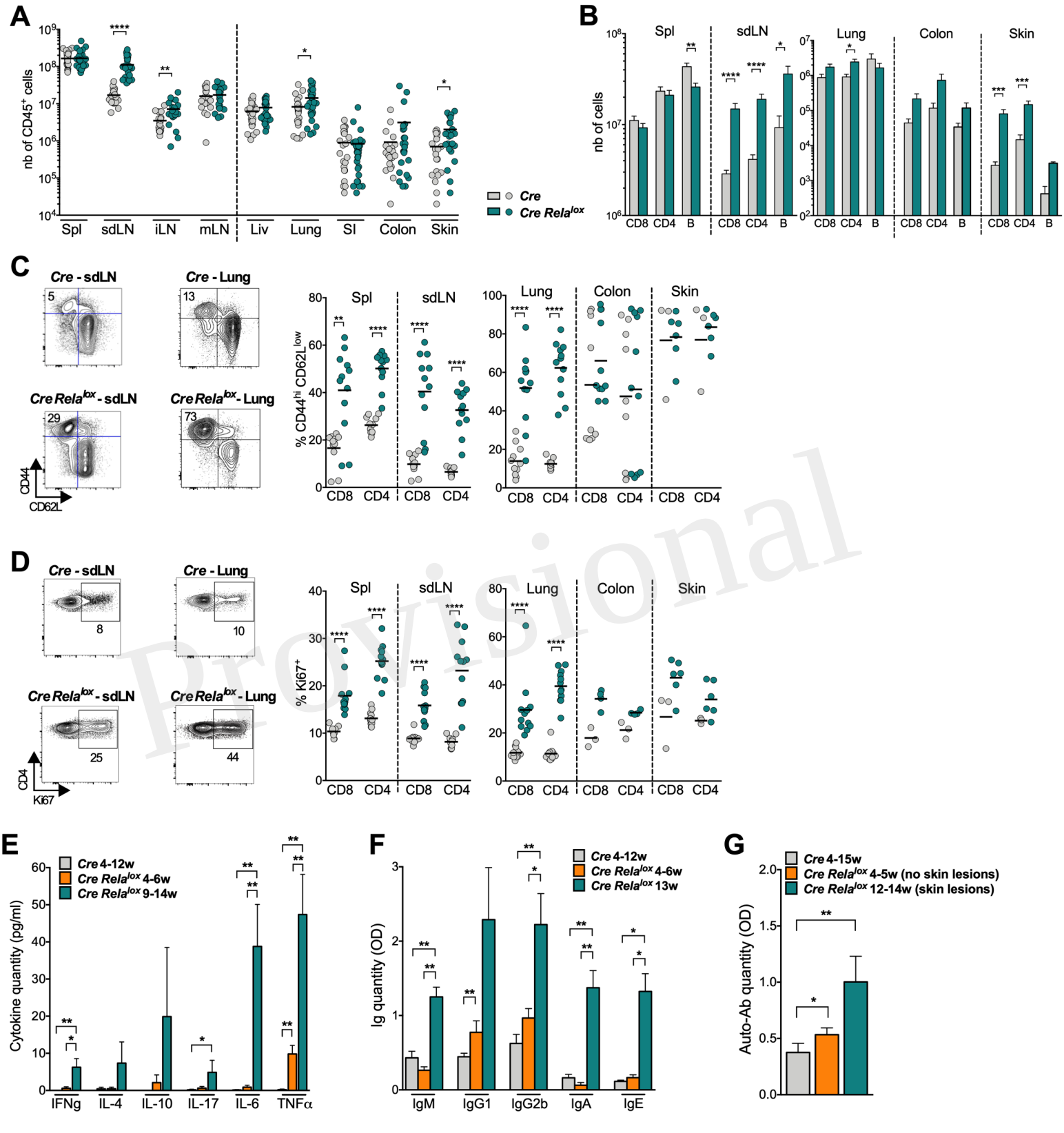

Figure 03.TIFF

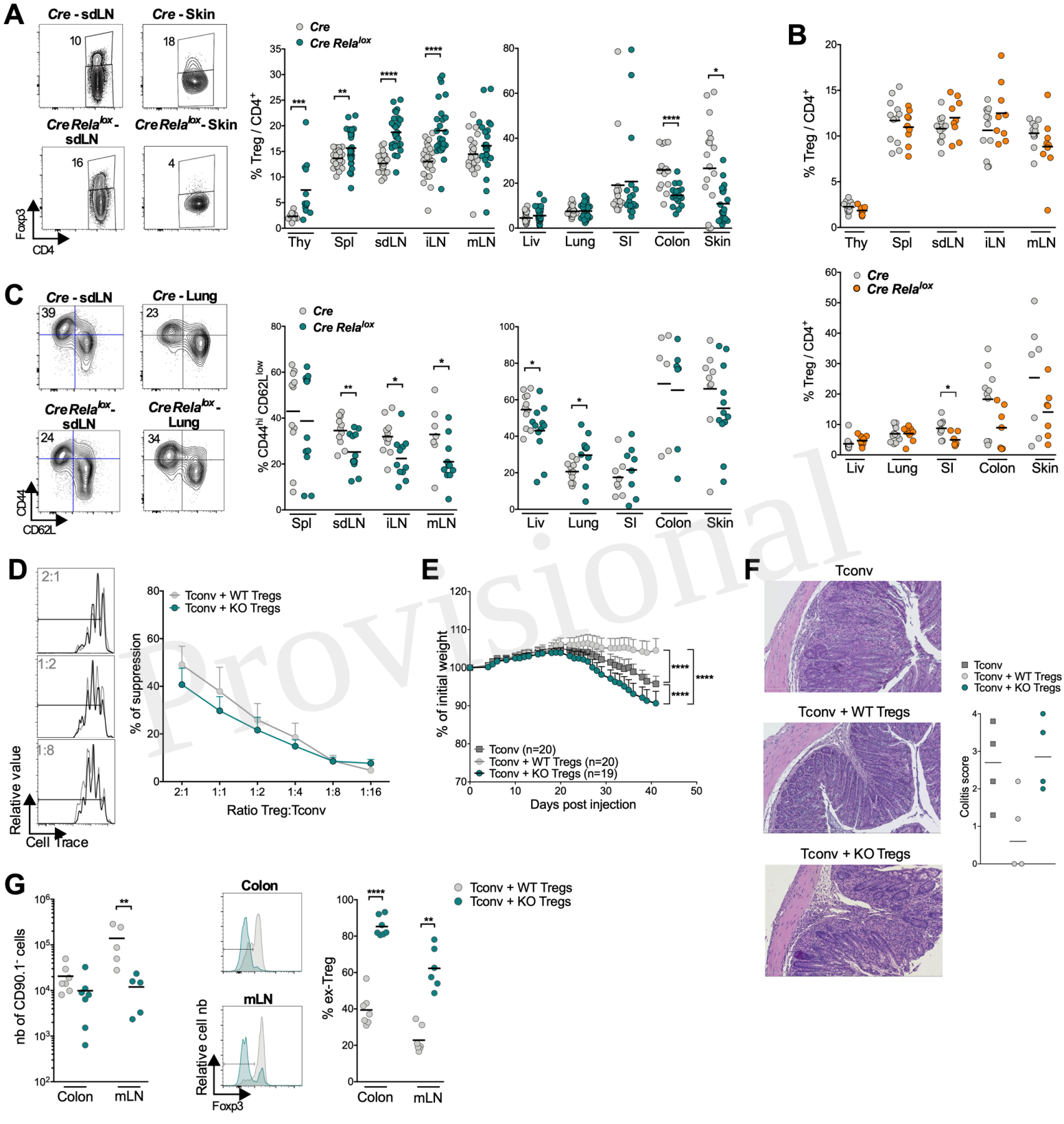

Figure 04.TIFF

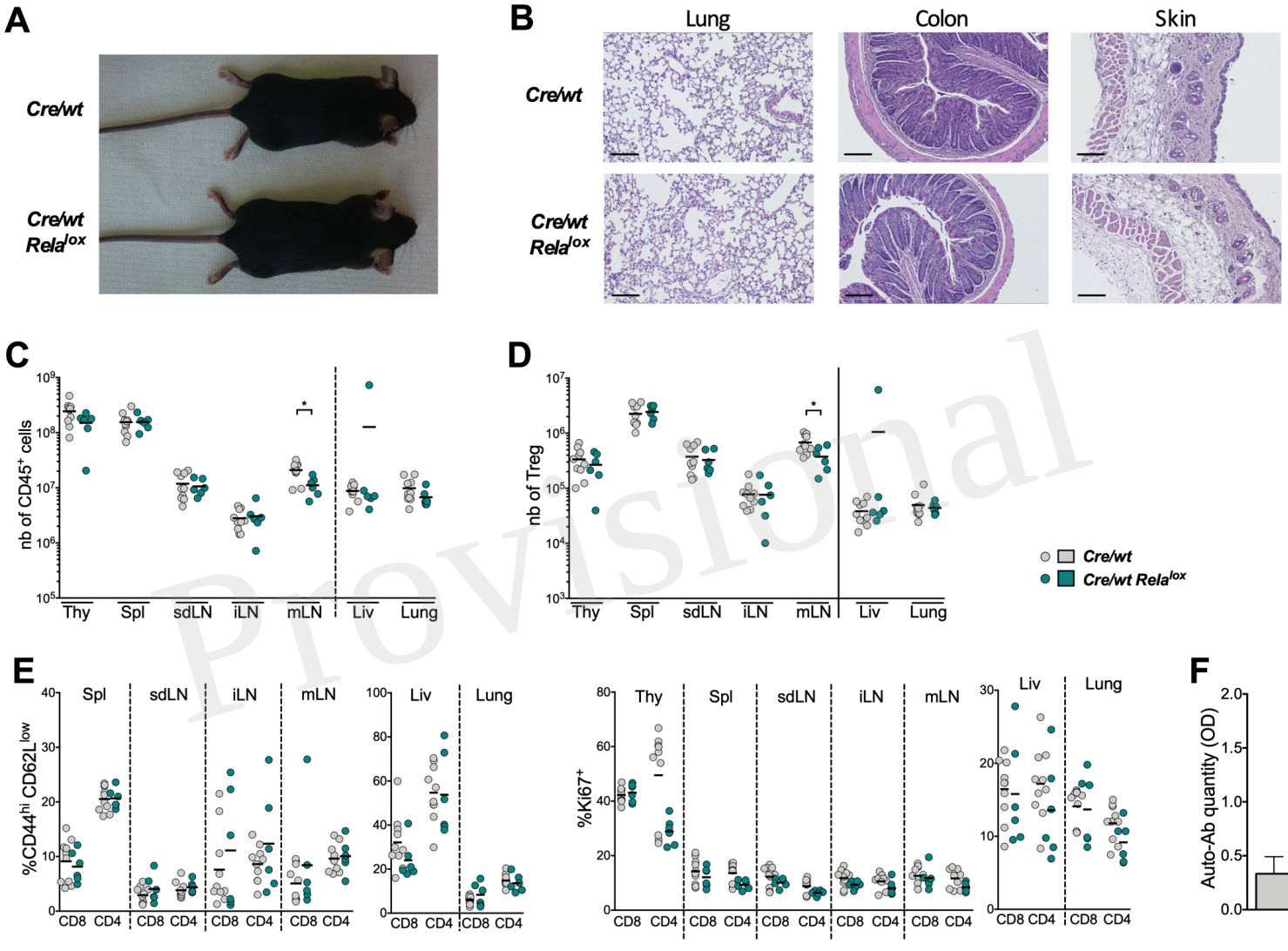

Figure 05.TIFF

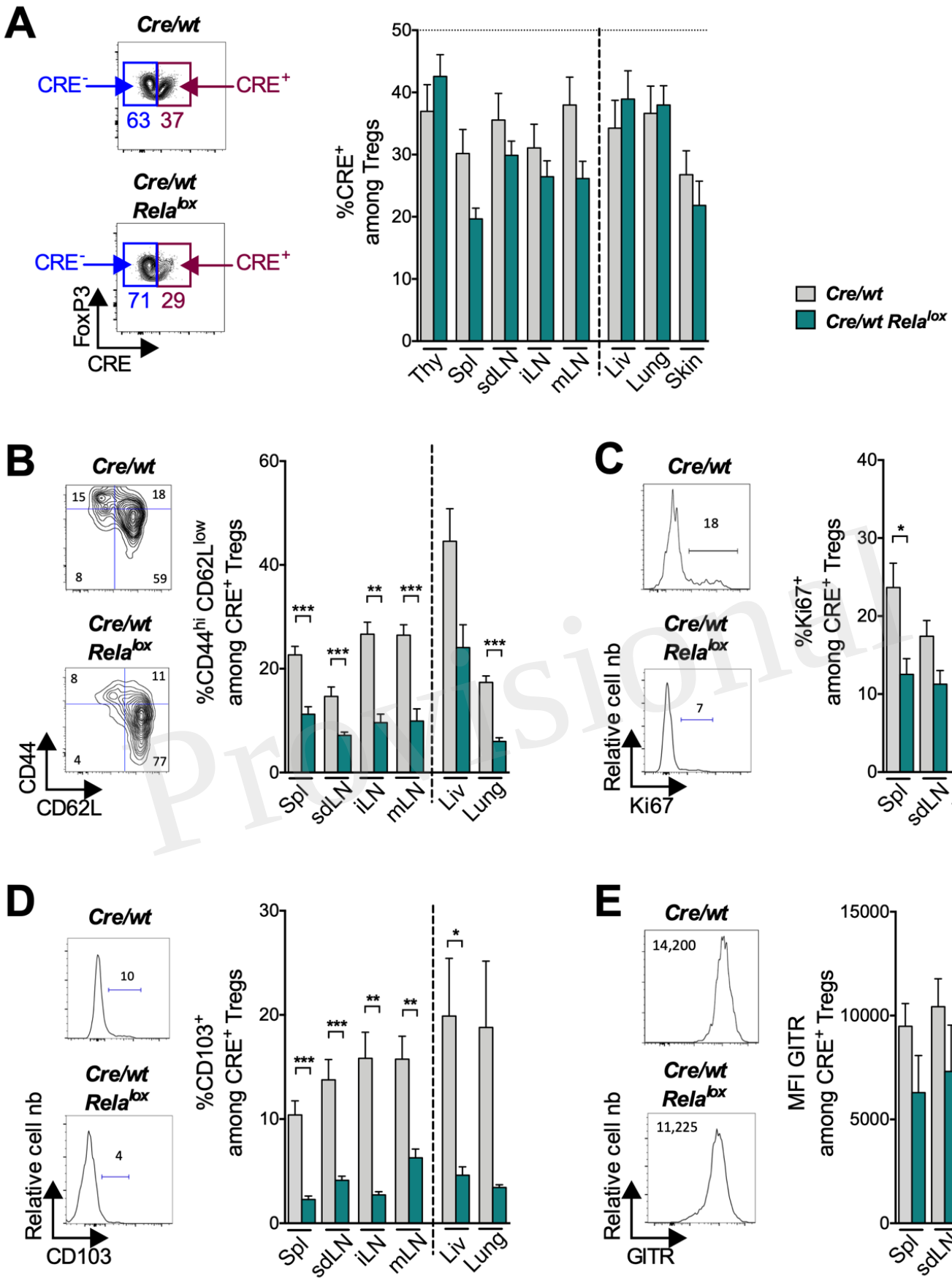

Figure 06.TIFF

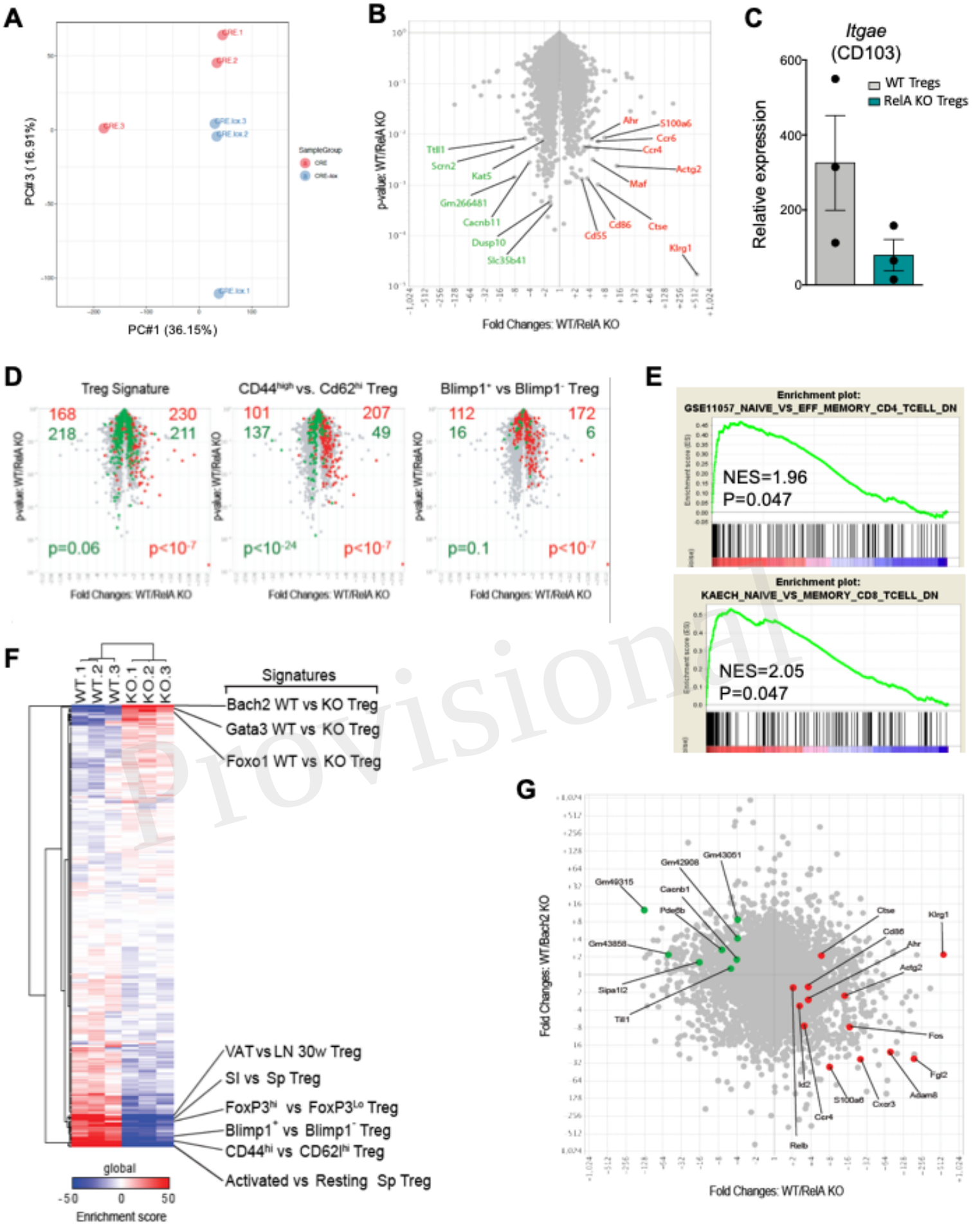

Figure 07.TIFF